1   Development

Literature:

Geometry: Consider an ultrafast pump-probe scattering experiment (See Figure 1 for an example and definitions of lab-frame coordinates). For today, we will take the pump to be an optical ultrafast pulse. This pump strikes an isotropic sample (e.g., provided by a gas jet) at $t = 0$, and promotes a (hopefully) single-photon transition in some of the sample molecules from the stationary Frank-Condon state S_0 to an excited state S_N, setting up non-adiabatic dynamics. Single-photon absorption is not isotropic, but proportional to the square of the $\hat{z}$ component of the transition dipole moment at the Frank-Condon point. At time delay t, the scattering probe (x-ray or electrons, depending on the experiment) strikes the sample, and takes a snapshot of the current geometry of the sample in terms of the scattering pattern on the detector. Typically, this signal is adjusted by subtracting the $t = -\infty$ signal, exposing changes in the geometry for the pumped molecule, and providing a "molecular movie" if a number of pump-probe time delays are sampled. Note that the subtraction of the $t = -\infty$ component of the signal serves to remove the scattering signal from the non-excited molecules (which remain in the time-independent steady-state FC wavepacket).
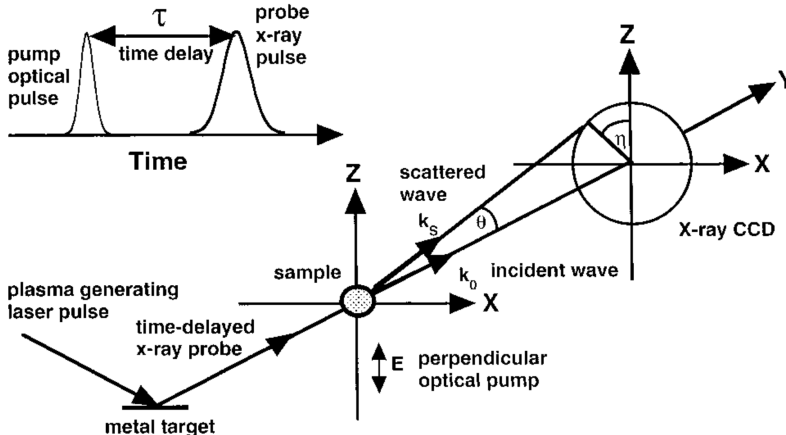

Figure 1: An illustration of ultrafast X-ray diffraction (along with UED, this is one of the main types of pump-probe scattering experiments that we consider). The X-ray probe arrives a delay of t with respect to the optical pump. In the perpendicular experimental arrangement (shown here), the polarization vector $\vec{E} \propto \hat{z}$ of the optical pump pulse is perpendicular to the incident wave vector $\vec{k}_0 \equiv k\hat{y}$ of the X-ray probe pulse. The incident X-ray photons scatter at angle θ with respect to $\vec{k}_0$, and azimuthal angle η with respect to $\vec{E}$. These two angles fully describe the scattering in the elastic regime, as $|\vec{k}_0| = |\vec{k}_s|$. The scattering vector $\vec{s}$ is the difference between the incident and scattered wave vectors $\vec{s} \equiv \vec{k}_0 - \vec{k}_s$. The amplitude of the scattering vector is $s \equiv |\vec{s}| = 2k \sin \theta/2 = (4\pi/\lambda) \sin \theta/2$. Figure adapted to our notation from Kent Wilson's excellent 1998 ultrafast scattering paper in JPCA [Jianshu Cao and Kent R. Wilson, *J. Phys. Chem. A* **102**, 9523 (1998)].

Objective: As theorists, our objective is to perform a computational simulation of the non-

adiabatic dynamics and time-resolved scattering signal observable of the ultrafast pump-probe experiment. To make things easy, let us assume that we have performed the non-adiabatic dynamics simulations, and have a representation for the density of the wavepacket in terms of a set of weighted trajectories $\{r_A^I(t), w_I(t)\}$. Each density-matrix trajectory basis function (e.g., a pair of AIMS TBFs in the Mulliken or saddle-point approximation, or an adiabatic trajectory) has a set of time-dependent nuclear coordinates $r_A^I(t)$, a time-dependent weight factor $w_A(t)$, which accounts for the weight of the starting configuration in the Franck-Condon point (Wigner sampling provides even weights, but there may also be weights due to sampling from different conformers), the overall oscillator strength, and any changes in weights due to adiabatic state population changes over the dynamics, and an adiabatic electronic label often denoted as $|I\rangle$.

We also apply one additional convention (not usually seen in AIMS) to our trajectories: we assert that the transition dipole moment of the $t = 0$ frame is aligned to $\hat{z}$, and that all subsequent frames follow this lab frame alignment. This will allow for the efficient treatment of anisotropic absorption later, by "reusing" each trajectory many times with different orientations. Note that this convention can be applied *after* running AIMS, by rotating all frames of a given trajectory tree by the rotation matrix to bring the $t = 0$ frame into the $\hat{z}$ axis.

In particular, our job is to produce the time-dependent detector pattern $I(\theta, \eta, t)$, the detector moments $I_l(\theta, t)$, and the corresponding radial distribution functions $I_l(r, t)$.

Elastic Scattering: We will assume we are working in the elastic scattering regime (no momentum transfer to the sample), which implies that $|\vec{k}_0| = |\vec{k}_s|$. This constraint reduces the dimensionality of the valid scattering space by 1.

$$\vec{s} = s\{\cos\theta/2\sin\eta, \sin\theta/2, \cos\theta/2\cos\eta\}$$

Here $s = 2k\sin\theta/2 = (4\pi/\lambda)\sin\theta/2$. Because of this relationship, s and θ are used interchangably in discussing the scattering.

IAM: In the independent atom model (IAM), the scattering for a given molecular "frame" I, with known and fixed orientation, is,

$$I_I(\vec{s}, t) = \left| \sum_A f_A(s) e^{i\vec{s}\cdot\vec{r}_A^I(t)} \right|^2$$

The spherically-isotropic atomic form factors are available for X-ray scattering and UED from considerations of the atomic electronic density (see below), or may be computed from scattering codes like ELSEPA (specialized for UED).

The total scattering signal is computed as,

$$I(\vec{s}, t) = \sum_I w_I(t) \int_{SO(3)} d\hat{R} \ \hat{R}_{zz}^2 \left| \sum_A f_A(s) e^{i\vec{s}\cdot\hat{R}\vec{r}_A^I(t)} \right|^2 / \int_{SO(3)} d\hat{R}$$

Note the "smearing" over all sample orientations $\hat{R}$, with $\hat{R}_{zz}^2$ weight for the anisotropic absorption.

Note that,

$$\int_{SO(3)} d\hat{R}\ \hat{R}_{zz}^2 / \int_{SO(3)} d\hat{R}\ = \frac{1}{3}$$

Detector Signals: The detector signal can be expanded as,

$$I(\vec{s}, t) = \sum_I w_I(t) \sum_{A,B} f_A(s) f_B(s) K_{AB}(\vec{s}, t)$$

where,

$$K_{AB}(\vec{s}, t) = \int_{SO(3)} d\hat{R}\ \hat{R}_{zz}^2 e^{i\vec{s}^\dagger \hat{R} \vec{r}_{AB}^I(t)} / \int_{SO(3)} d\hat{R}$$

The rotation group integrals are worked out in A. H. Zewail and J.S. Baskin, *Chem. Phys. Chem.*, **6**, 2261 (2015). For the perpendicular case (selection weight of $\hat{R}_{zz}^2$):

$$K^\perp(\vec{s}) = \frac{J_1(sr)}{sr} - \left[\sin^2\gamma + (2 - 3\sin^2\gamma)\cos^2(\theta/2)\cos^2\eta\right]\frac{J_2(sr)}{2}$$

For the parallel case: (selection weight of $\hat{R}_{yy}^2$):

$$K^\parallel(\vec{s}) = \frac{J_1(sr)}{sr} - \left[\sin^2\gamma + (2 - 3\sin^2\gamma)\sin^2(\theta/2)\right]\frac{J_2(sr)}{2}$$

For the isotropic case, (selection weight of 1):

$$K^\emptyset(\vec{s}) = J_0(sr)$$

In the above $\gamma = \cos^{-1}(\hat{r} \cdot \hat{z})$ and $r = |\vec{r}|$. Note that $\sin^2\gamma = 1 - (\hat{r} \cdot \hat{z})^2 = 1 - r_z^2/r^2 = (r_x^2 + r_y^2)/r^2$.

The spherical Bessel functions are,

$$J_0(s) = \frac{\sin x}{x}\ : 1$$

$$J_1(x) = \frac{\sin x}{x^2} - \frac{\cos x}{x}\ : 0$$

$$J_2(x) = \left(\frac{3}{x^2} - 1\right)\frac{\sin x}{x} - 3\frac{\cos x}{x^2}\ : 0$$

The limits at $x = 0$ are displayed. Also note that $\lim_{x\to 0} J_1(x)/x = 1/3$.

Modified Diffraction Intensity: Particularly for UED, the raw diffraction intensity above is too peaked near the origin. To facilitate analysis, a "modified" diffraction intensity is often defined as,

$$sM(s) \equiv s\frac{I_{\mathrm{mol}}(s)}{I_{\mathrm{at}}(s)}$$

Here, the atomic contribution of the scattering is,

$$I_{\mathrm{at}}(s) \equiv \sum_A |f_A(s)|^2$$

Note that this is time and structure invariant. The molecular scattering signal is,

$$I_{\mathrm{mol}}(s) \equiv I(s) - F I_{\mathrm{at}}(s)$$

Here $F = 1/3$ for perpendicular and parallel transitions, $F = 1$ for isotropic transitions.

Anisotropy: For a perpendicular pump-probe arrangement, the scattering signal can be exactly decomposed into,[1]

$$I(s, \eta, t) = I_0(s, t) + I_2(s, t) \cos(2\eta)$$

This decomposition can be computed from two collocation points as,

$$I_0(s, t) = \frac{1}{2} \left[I(s, \eta = 0, t) + I(s, \eta = \pi/2, t) \right]$$

$$I_2(s, t) = \frac{1}{2} \left[I(s, \eta = 0, t) - I(s, \eta = \pi/2, t) \right]$$

Pair Correlation Functions: The distance pair correlation is computed from the UED detector signal as,

$$M(r, t) \equiv \int_0^{s_{\max}} \mathrm{d}s \; s M(s) \sin(sr) \exp(-\alpha s^2)$$

Formally, $s_{\max} \to \infty$ for an exact sine transform. In practice, a cutoff must be used due to the outer limits of s values that are scattered. The cutoff function $\exp(-\alpha s^2)$ is used to damp down noise from large s. Additionally, the detector signal is only available from $s_{\min}$ and up, so the signal is typically assumed to rise smoothly[2] from $s = 0$ to the value at $s_{\min}$.

Typically this analysis is applied to the isotropic difference signal $\Delta M_0(s, t) = M_0(s, t) - M_0(s, t = -\infty)$.

Specific Example I: UED at SLAC: One of the main experiments we are trying to support is the UED-III endeavor at SLAC. A representative paper of the approach and setup is from the UED-I run: J. Yang et al, *Nat. Comm.*, **7**, 11232 (2016). Another good paper is on the instrument design: S. Weathersby et al, *Rev. Sci. Instr.*, **86**, 073702.

In this experiment, 3.7 MeV electrons are used as the probe ($\lambda = 0.30$ pm $= 0.0030$ Å). The detector is an Andor iXon ultra 888 electron multiplying charge-coupled device camera (EMCCD), which is positioned 3.1 m from the sample. The accessible range of s is 3.5 Å^{-1} to 12 Å^{-1}, corresponding to scattering angles θ of 0.0957° to 0.328°, or a detector radius of

---

[1]Note that everyone seems to be using Legendre polynomials in the literature. This doesn't make sense to me, and I have empirical evidence that the scattering signal exactly decomposes onto 1 and $\cos(2\eta)$ azimuthal basis functions for $\hat{R}_{zz}^2$ anisotropy.

[2]Linearly?

s_z of 0.52 to 1.78 cm. Large s is limited by the size of the detector, small s is limited by the 0.4 cm diameter hole drilled in the EMCCD for the electron beam (thought this may be improved in later runs). Note that this is very small angle scattering, but permits rather high values of s due to the small deBroglie wavelength of ultra-relativistic electrons. By contrast, x-rays typically scatter over much larger angles to reach similar values of s. For instance, 1.3 Å wavelength electrons reach only $s = 9.7$ Å^{-1} over the entire scattering sphere.

In analysis, the UED team typically uses a cutoff of $\alpha = 7^{-2}$ Å^{-2} in the sine transform above.

The entire instrument has a time resolution of roughly 100 fs, and notably lacks an in-flight diagnostic clock (e.g., "timestamping"), though a THz streaking experiment has recently been developed to provide an offline clock calibration.

A Ti:Sapphire laser serves as both pump and probe initiator. Part of the laser pulse initiates electron release from a copper photocathode (photoelectron release), which are subsequently accelerated to 3.7 MeV by a massive klystron. Tilting/tuning the klystron accelerates the back of the electron bunch more than the front, combating Coulomb spread in the probe electron bunch, but this can induce problems in determining the time delay.

X-Ray Scattering vs. Electron Diffraction: For ultrafast x-ray scattering, the form factors $f_A(s)$ are the Fourier transform of the electronic density of a spherical atom (possibly selected to reflect the density of the local chemical environment in the true molecule),

$$f_A(s) \equiv \int_{\mathbb{R}^3} dr_1 \; \rho_A^{\mathrm{e}}(\vec{r}_1) e^{i\vec{s}\cdot\vec{r}_1}$$

These form factors are tabulated for many common atoms at

```
http://lampx.tugraz.at/~hadley/ss1/crystaldiffraction/
atomicformfactors/formfactors.php
```

(accessed 01/18/2018). The specific parametrization is,

$$f_A(s) \equiv \sum_{i=1}^{4} a_i \exp\left(-b_i \left(\frac{s}{4\pi} \right)^2 \right) + c$$

With 9 parameters a_{1-4} b_{1-4}, and c per atom type. Units are Å^{-1}.

To switch to ultrafast electron diffraction, one must also account for scattering off of the nucleus and for a modified Jacobian element,

$$f_A^{\mathrm{UED}}(s) \equiv \frac{1}{s^2} \left[Z_A - f_A^{\mathrm{XRAY}}(q) \right]$$

See M. Ben-Nunn, J. Cao, and K. Wilson, JPCA, 101, 8744 (1997) for details.

2   Example: Iodine

Geometry: As a key example, we consider a perpendicular pump-probe UED experiment wherein iodine molecule I_2 is excited to a hypothetical bound state via a parallel transition (transition dipole along the molecular axis).[3] The classical trajectory is,

$$r(t) = 2.66 + 0.5\sin(2\pi t[\text{fs}]/600)[\text{Å}]$$

Using the techniques above, we compute the detector moments $I_0(s,t)$ and $I_2(s,t)$ for each of the frames in the trajectory (see Figure 2). We use the accessible range of $s \in [3.5, 12.0]$ Å^{-1} for the UED experiment, and use a de Broglie wavelength of $\lambda = 0.0030$ Å, which corresponds to the 3.7 MeV electrons of the experiment.
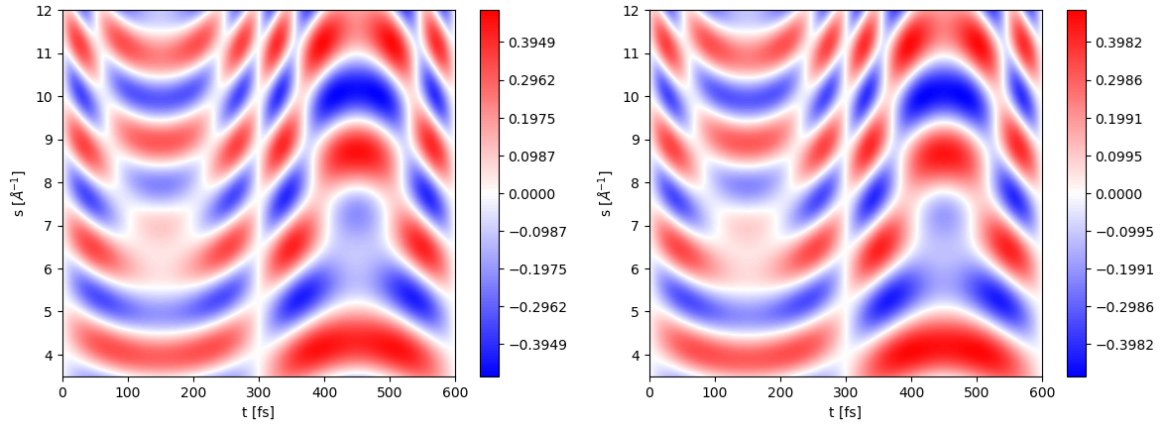

Figure 2: Detector moments $I_0(s,t)$ and $I_2(s,t)$ for toy iodine problem. These moments are differences (as are all plots in this section), i.e., $I(s,t) \leftarrow I(s,t) - I(s,t=0)$. These moments are of the flavor $sM(s,\eta,t)$ (as are all plots in this section).

At this point, we can easily compute the detector patterns from $I(s,\eta,t) = I_0(s,t) + I_2(s,t)\cos(2\eta)$. E.g., an interesting frame is $t = 132$ fs, and the decomposition into isotropic/anisotropic parts is also shown. A complete 3D detector movie over (s,η,t) is in `figs/i2-movie` in this TeX source dir.

Starting from the moments, e.g., $I_0(s,t)$, we can compute the "molecular movie" $I_0(r,t)$ by sine transforming. This is done in Figures 4 and 5 for our toy iodine problem, using a variety of $s_{\min}$ and $s_{\max}$ cutoffs, and without/with time blurring with a 100 fs FWHM Gaussian. The upper right figure in Figure 4 shows roughly what can be expected with the current experimental setup.

Of particular note, the $s_{\min}$ limit due to the hole for the electron beam induces large "fringes" in the signal. It might be plausible that pushing $s_{\min}$ down could be just as useful as pushing $s_{\max}$ up in cleaning up these pictures.

---

[3]Note that this toy problem is chosen for ease of setup/representative nature, not for rigorous physics.
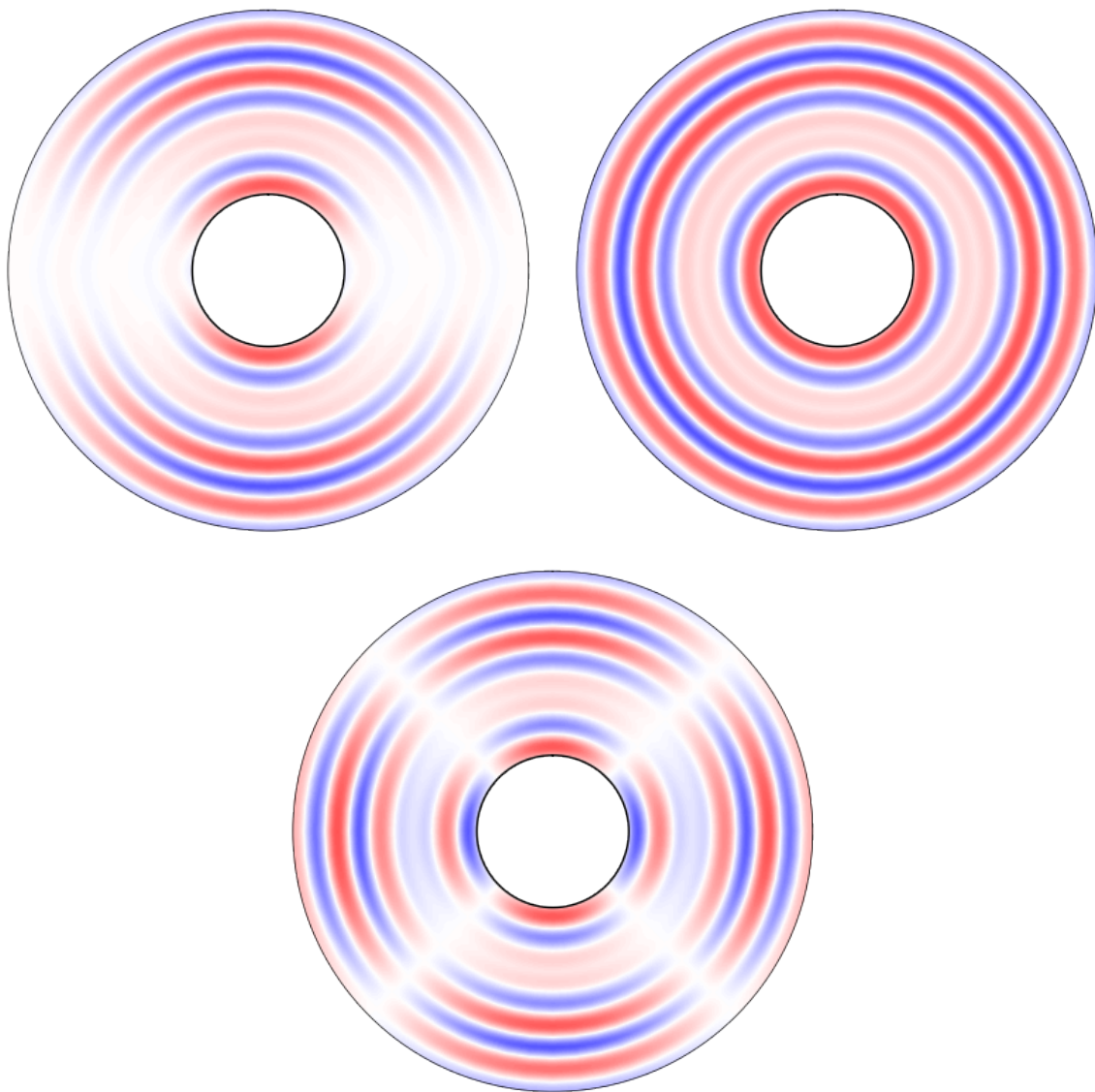
Figure 3: Detector patterns $I(s, \eta)$, $I_0(s, \eta)$ and $I_2(s, \eta)$ for toy iodine problem ($t = 132$ fs).
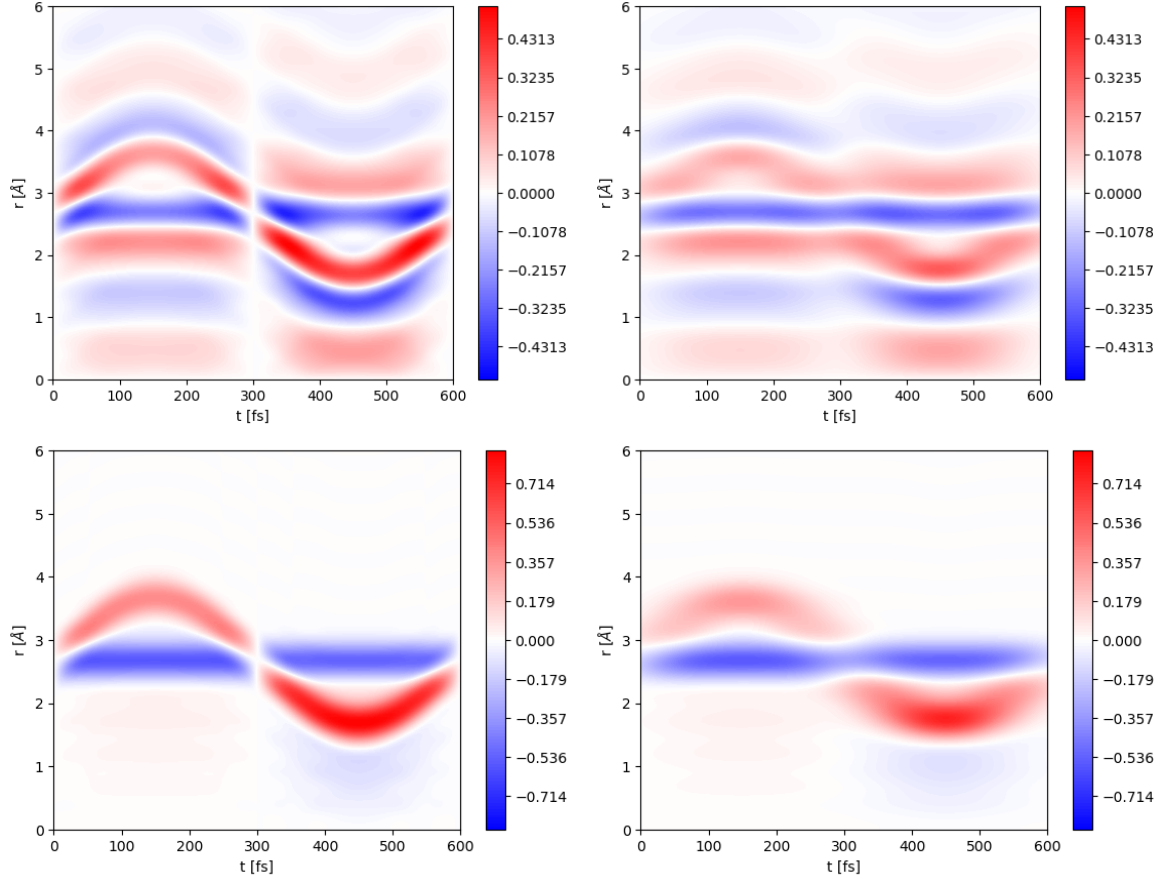
Figure 4: Molecular movies $I_0(r, t)$ for toy iodine problem. On the left is the 1 fs resolution signal. On the right is the 100 fs FWHM time-blurred system (Gaussian blurring). On the top, the $s_{\min} = 3.5$ Å^{-1}. On the bottom, $s_{\min} \sim 0.0$ Å^{-1}. In all cases, $s_{\max} = 12.0$ Å^{-1}.
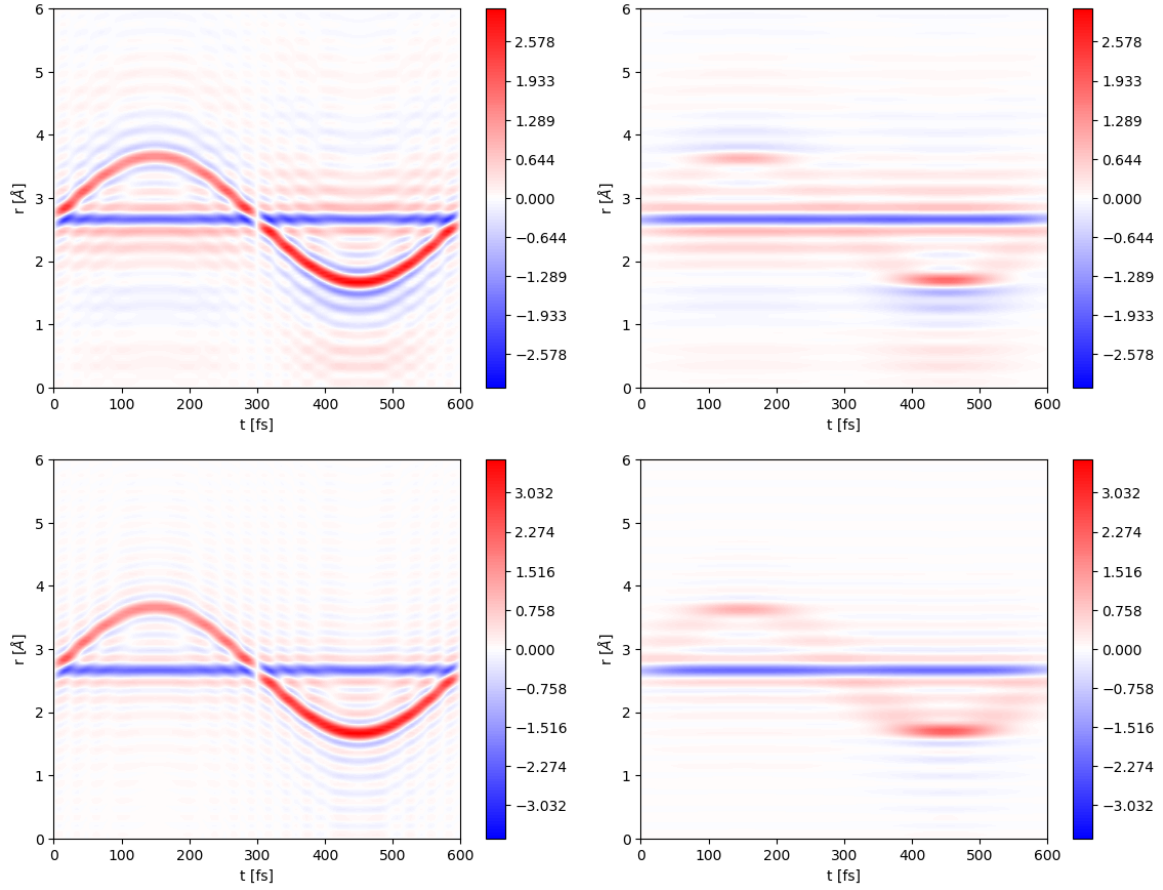
Figure 5: Molecular movies $I_0(r, t)$ for toy iodine problem. On the left is the 1 fs resolution signal. On the right is the 100 fs FWHM time-blurred system (Gaussian blurring). On the top, the $s_{\min} = 3.5$ Å^{-1}. On the bottom, $s_{\min} \sim 0.0$ Å^{-1}. In all cases, $s_{\max} = 24.0$ Å^{-1}. Note that $\alpha = 0$ in the sine transform in this case.